Climate state dependent response to high-latitude effusive volcanic eruptions

Tómas Zoëga[1], **Trude Storelvmo**[1], **Kirstin Krüger**[1]

[1]Department of Geosciences, University of Oslo, Oslo, Norway

Key Points:

- Arctic winter warming due to effusive volcanic eruptions is amplified under pre-industrial climate compared to the present day and future.
- Arctic summer cooling increases with warming climate due to decreased sea ice. This is despite stronger cloud response in colder climates.
- Increased cloud shielding induced by volcanic aerosols significantly increases summer sea ice area in the Arctic across climate states.

Corresponding author: Tómas Zoëga, `tomas.zoega@geo.uio.no`

Abstract

Effusive volcanic eruptions have been common in Iceland throughout the Holocene with the largest ones happening prior to the industrial revolution. Such eruptions can affect climate through the formation of sulfate aerosols and subsequent impacts on clouds. As different atmospheric conditions modulate the cloud and climate responses to aerosol perturbations, a pre-industrial effusive eruption might have different climate impacts were it to happen today or in the future. Here we use an Earth system model to simulate the surface climate response to Icelandic effusive volcanic eruptions under pre-industrial, present day, and end of the 21st century climate conditions. For the last case, high anthropogenic greenhouse gas and aerosol emissions are assumed. We find that the climate state significantly modulates the climate response, especially in the Arctic where we model amplified surface warming during winter under pre-industrial conditions and stronger surface cooling during summer in warmer climates.

Plain language summary

Effusive volcanic eruptions are relatively gentle compared to explosive eruptions, resembling boiling stews rather than fireworks. They often last weeks, or even years, and can emit large amounts of gases into the lower atmosphere. Among them is sulfur dioxide, which is quickly turned into small particles called aerosols. When these aerosols enter clouds, they can change the interactions between the clouds and radiation, thereby impacting climate. Prior to the industrial revolution, the atmosphere was cleaner than it is today due to less human influence. Since clouds react differently to aerosol perturbations depending on the background aerosol level, we would expect stronger climate impacts from pre-industrial effusive eruptions. Here we use an Earth system model and find that this is indeed the case. We find that pre-industrial effusive eruptions would have led to greater increase in reflected sunlight, compared to present day and future eruptions, leading to stronger surface cooling during summer. We also find a greater increase in the ability of pre-industrial Arctic clouds to trap thermal emissions close to the ground, leading to stronger pre-industrial surface warming during winter.

1 Introduction

Effusive volcanic eruptions have been common in Iceland throughout the Holocene (Sigl et al., 2022). The largest took place prior to the first industrial revolution, with notable examples including the 939-940 Eldgjá (Thordarson et al., 2001; Oppenheimer et al., 2018) and 1783-84 Laki (Thordarson & Self, 2003) flood lava eruptions. Effusive eruptions are among the strongest natural sources of atmospheric sulfur as they release large amounts of sulfur dioxide (SO_2), a precursor gas to sulfate (SO_4) aerosols, over extended periods of time (Bates et al., 1992). Through these emissions, effusive eruptions can significantly impact clouds and climate (e.g., Yuan et al., 2011; Malavelle et al., 2017; Breen et al., 2021; Chen et al., 2022; Zoëga et al., 2023).

SO_4 aerosols are known to be effective cloud condensation nuclei (CCN). By providing more opportunities for cloud droplets to form, they lead to increased cloud shortwave (SW) albedo through the formation of more numerous but smaller cloud droplets (Twomey, 1977). Depending on the atmospheric conditions, smaller droplets can either hinder precipitation, leading to longer cloud lifetimes with increased cloud liquid water content and greater cloud cover (Albrecht, 1989; Chen et al., 2022; Murray-Watson & Gryspeerdt, 2022; Wang et al., 2024), or they can lead to quicker evaporation, hence shortening the cloud lifetime (Small et al., 2009; Toll et al., 2019). These aerosol-cloud interactions, often referred to as the cloud albedo effect and the cloud lifetime effect respectively, greatly impact the Earth's climate by modulating radiative forcing (Lohmann & Feichter, 2005). Additionally, SO_4 aerosols interact directly with radiation, mainly by scattering sunlight (Li et al., 2022).

Clean clouds react stronger to aerosol perturbations than polluted clouds (e.g., Lohmann & Feichter, 2005). Considering how anthropogenic aerosols make up a substantial portion of the present day atmospheric aerosol column burden (e.g., Satheesh & Moorthy, 2005), this implies that clouds during the relatively unpolluted pre-industrial era were more susceptible to volcanic aerosol perturbations than they are today. Using an aerosol microphysics model embedded in a chemical transport model, Schmidt et al. (2012) found that the global mean cloud droplet number concentration responded considerably stronger to volcanic degassing of SO_2 under pre-industrial conditions compared to the present day, accompanied by a stronger cloud albedo increase.

Here, we investigate how the climate state modulates the climate response to long lasting, Icelandic effusive volcanic eruptions using an Earth system model. We focus on three different climate states. One corresponding to the pre-industrial era, characterized by limited anthropogenic influences; a second one corresponding to the present day, with higher background aerosol load and tropospheric temperatures as a result of human activities; and a third corresponding to the climate at end of the 21st century under the assumption that both anthropogenic greenhouse gas and aerosol emissions remain high throughout the century.

2 Methods

2.1 Model

In this study, we use the Community Earth System Model version 2.1.3 with the Community Atmosphere Model version 6, abbreviated as CESM2(CAM6) (Danabasoglu et al., 2020). CESM2(CAM6) includes the Modal Aerosol Model (MAM4) (Liu et al., 2016), which simulates tropospheric aerosols, and the prognostic Morrison-Gettelman cloud microphysics scheme version 2 (MG2) (Gettelman & Morrison, 2015). The oxidants ozone (O_3) and the hydroxyl radical (OH), along with stratospheric aerosols, are prescribed from CMIP6 simulations using the Whole Atmosphere Community Climate Model (WACCM) (Gettelman et al., 2019). CESM2(CAM6) extends to an altitude of 2.26 hPa, amounting to ca. 40 km, and includes 32 vertical levels. We use a horizontal resolution of 0.9° latitude by 1.25° longitude. The sea ice model, CICE version 5.1.2 (Hunke et al., 2013; Danabasoglu et al., 2020), includes interacting components of sea ice thermodynamics, dynamics, transport, and parameterized ridging. In our simulations, atmospheric, sea ice, oceanic, and land components are all active and coupled.

2.2 Experimental design and data processing

We use CESM2(CAM6) to model the climate response to high-latitude effusive volcanic eruptions under pre-industrial (PI), present day (PD), and future (Ft) climate conditions. For each of these climate states, we carry out a ten year long control run. On June 1st and December 1st of each year, we branch a simulation off from these controls and add a volcanic eruption. Each of those eruption branch simulations is six months long. We perform a pairwise comparison where each eruption branch is compared to the corresponding part of the corresponding control, resulting in sets of ten anomalies for each of the climate states. These sets, or ensembles, of anomalies form the basis of our analysis. This approach is termed a matched-pairs analysis (e.g., Barlow, 1993). We calculate 95% confidence intervals around the ensemble means based on a two-tailed *t*-test.

2.3 Climate states

To simulate different climate states, we start from CESM2 Coupled Model Intercomparison Project Phase 6 (CMIP6) simulations (Eyring et al., 2016) and fix greenhouse gas concentrations, atmospheric oxidants, stratospheric ozone and stratospheric aerosols, along with natural and anthropogenic aerosol and aerosol precursor emissions, to a particular year. This year is 1850 in the PI simulations, 2010 in the PD simulations, and 2090 in the Ft simulations. To represent the future in the Ft simulations we use the shared socioeconomic pathway (SSP) SSP3-7.0 (O'Neill et al., 2016). The rationale behind this choice is that in SSP3-7.0 both greenhouse gas and aerosol emissions remain high throughout the century. This is different from the other SSP scenarios used in CMIP6 where aerosol emissions decrease (Shiogama et al., 2023). Also, the Arctic is virtually ice free at the end of the melt season under SSP3-7.0 conditions at the end of the 21st century.

2.4 Volcanic emissions

The volcanic eruptions in our simulations last for six months, are represented by prescribed SO_2 emissions, and are well mixed between 1 and 3 km above sea level. Daily SO_2 emissions are constant within each month and amount to 2.5 Tg/day for the first month of the eruption, 1.625 Tg/day for the second month, 1.25 Tg/day for the third month, and 0.875 Tg/day for each of the remaining three months. Following Zoëga et al. (2024), this eruption scenario is based on the 2014-15 Holuhraun eruption in Iceland in terms of location (64.9°N, 16.8°W), emission altitude, duration, and how the emission strength decayed as the eruption went on (Thordarson & Hartley, 2015). The major difference between the 2014-15 Holuhraun eruption and our eruption scenario is that our eruptions are ca. 25 times larger in terms of the SO_2 emission rate, rivaling the largest known effusive eruption in Iceland during the Holocene (Hjartarson, 1988; Bonny et al., 2018).

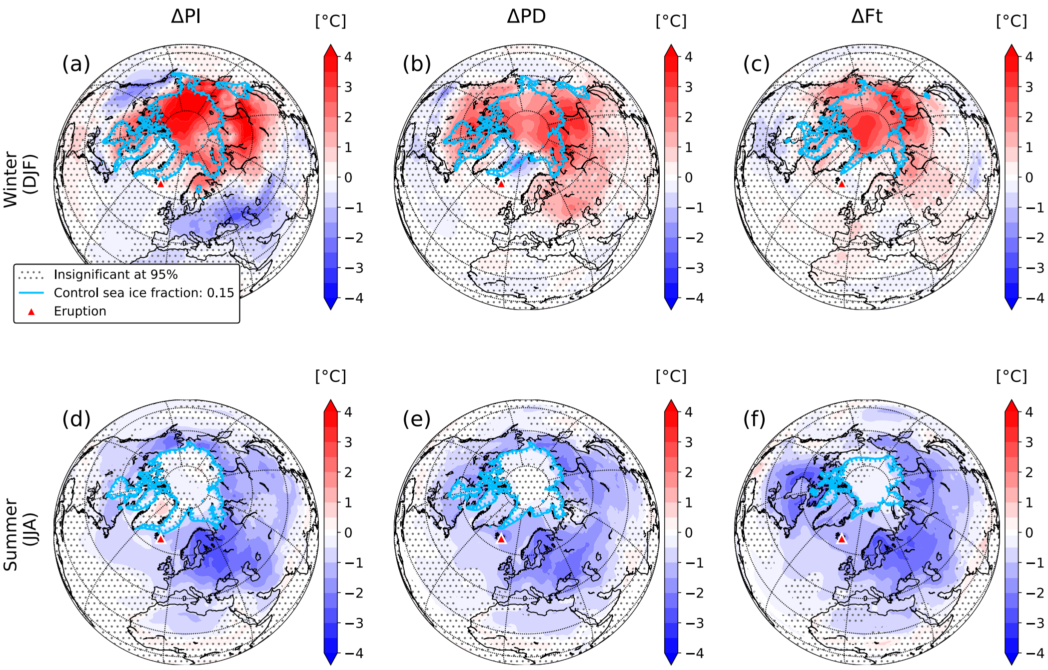

Figure 1. Ensemble mean surface air temperature anomalies for the first three months of eruptions starting in December (winter, upper panel) and June (summer, lower panel) under pre-industrial (PI; a and d), present day (PD; b and e), and future (Ft; c and f) conditions. Dotted regions indicate insignificance at the 95% confidence level using a two-tailed *t*-test. Light blue contours indicate control sea ice edge as defined by 15% sea ice fraction. Anomalies less than ±0.1°C are coloured white.

3 Results and discussion

3.1 Arctic response

3.1.1 Stronger surface winter warming under PI conditions

For eruptions starting in December, we model significant surface winter (December to February, DJF) warming across the Arctic (Figs. 1a to 1c) as a result of increased longwave (LW) radiation trapping by low level clouds under limited sunlight (Zoëga et al., 2023, 2024). The increased cloud cover (Fig. 2d) and thickness (Fig. 2c) are in turn caused by an increase in cloud droplets formed on volcanic SO_4 particles (Figs. 2a and 2b). This warming is significantly stronger in the PI simulations compared to the PD and Ft ones (Fig. 2f). The main reason concerns the background cloud states.

In general, the cloud liquid water path (LWP) is very low in the Arctic during winter. However, with warming climate we model a considerable increase in the background LWP going from PI to PD to Ft (Fig. 2i). Furthermore, once the LWP exceeds ca. 30 g/m^2, clouds become opaque to terrestrial LW radiation (Slingo et al., 1982; Shupe & Intrieri, 2004). Supplementary Fig. S1 shows how LWP $\leq$ 30 g/m^2 is widespread across the Arctic under unperturbed PI conditions, less prominent under PD conditions, and almost absent under Ft conditions. This results in a stronger PI warming, even though the LWP response is very similar between the different climate states considered (Fig. 2c). Less background low level cloud cover under PI and PD conditions compared to Ft conditions (Fig. 2j) facilitates greater horizontal spreading of clouds across otherwise clear skies (Fig. 2d), further contributing to the strong PI warming.

Earth system models tend to overestimate the LWP response to increased cloud droplet number concentration (N_d) on a global scale (e.g., Malavelle et al., 2017; Gryspeerdt et al., 2019). However, in a recent study, Murray-Watson and Gryspeerdt (2022) used satellite data to demonstrate a strong positive relationship between changes in N_d and LWP in the Arctic under high stability in the lower troposphere. Also using satellite data, Chen et al. (2022) and Wang et al. (2024) found a significant increase in cloud cover as a result of aerosol perturbations from a high-latitude effusive volcanic eruption, further supporting the plausibility of the cloud lifetime response in our simulations.

3.1.2 Summer cooling increases with less sea ice

As expected, the Arctic cloud response during summer (June to August, JJA) is stronger under the relatively clean PI conditions compared to the more polluted PD and Ft conditions (Figs. 2b to 2d) (e.g., Lohmann & Feichter, 2005). This translates into stronger PI decrease in net downward surface radiation (Fig. 2e). Despite this, we model the weakest Arctic mean surface cooling in the PI simulations and strongest in the Ft simulations (Fig. 2f).

As illustrated in Fig. 1, there is a general lack of surface air temperature response over the Arctic sea ice during summer. As discussed by Zoëga et al. (2024), the reason for this is twofold. On one hand is the decreased effectiveness of SW cloud shielding over sea ice due to multiple reflections between the clouds and the sea ice, both of which are characterized by high albedo (e.g., Wendler et al., 1981). On the other hand is reduced heat loss from the atmosphere to the sea ice in the case of an eruption due to less sea ice melting (Figs 3b and 3d). This limited temperature response over the Arctic sea ice holds especially true in the PI and PD simulations, where substantial sea ice cover is retained in the Arctic during summer (Fig. 3d). In the Ft simulations, where the summer sea ice cover is vastly reduced and virtually gone in early fall, we model a small but significant surface cooling across most of the central Arctic.

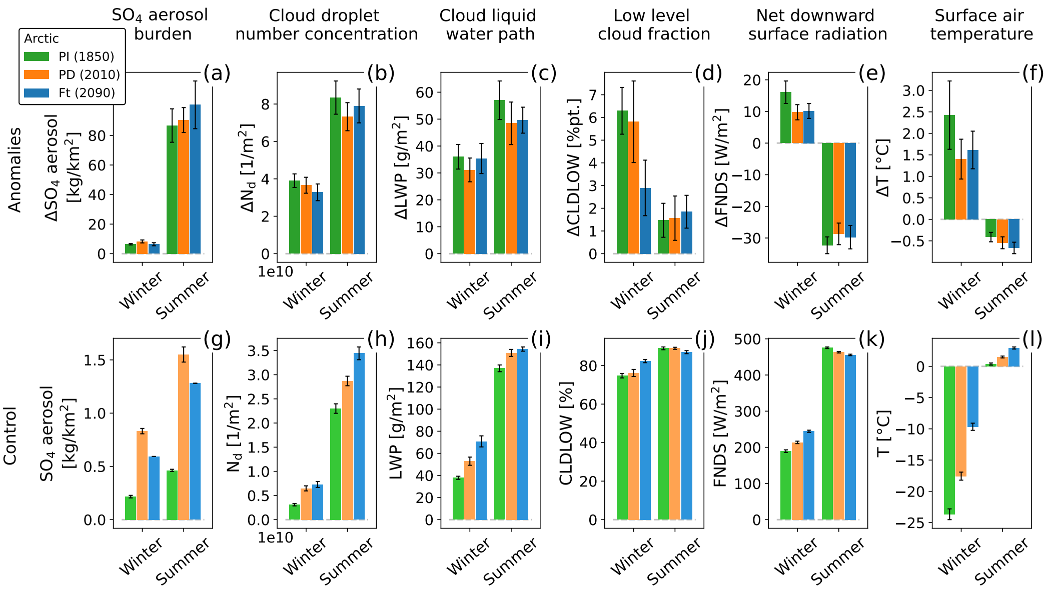

Figure 2. Arctic mean anomalies (upper panel) and corresponding controls (lower panel) for the first three months of eruptions starting in December (winter, DJF) and June (summer, JJA). Green bars indicate pre-industrial (PI) conditions, orange present day (PD), and blue future (Ft). Black bars indicate 95% confidence intervals based on a two-tailed *t*-test. Here, the Arctic is defined as the area north of 65°N, excluding landmasses.

3.1.3 Arctic sea ice area increases during summer across climate states

In addition to playing a major role in modifying the surface air temperature response, the Arctic sea ice area (defined as the sum of the sea ice covered area of all grid cells in the northern hemisphere which have ≥15% sea ice fraction, following Comiso et al. (2024)) is significantly impacted in our simulations.

While eruptions starting in December only marginally affect the wintertime Arctic sea ice, with anomalies mostly being insignificant (Figs. 3a and 3c), eruptions starting in June lead to significant increase in the summertime sea ice area (Figs. 3b and 3d). These positive anomalies are a result of reduced melt during summer and fall through increased SW cloud shielding. This is most prominent in the PD simulations where the June to November Arctic sea ice area in the eruption simulations approaches the corresponding PI control values (Fig. 3d). In both the PI and PD simulations, we model steadily larger sea ice area anomalies from the start of the summer eruption and into the fall before they start to wane. The temporal behaviour of the Ft response is different as we model a dip in the magnitude of the anomalies from August to October (Fig. 3b). The reason is that during these months, we model a virtually sea ice free Ft Arctic (Fig. 3d), hampering the formation of new ice through increased impacts of the ice-albedo feedback (e.g., Stroeve et al., 2012).

The greatest modelled increase in summer sea ice area, therefore, happens when partial background sea ice cover is maintained. When the ocean is either almost completely ice covered or when sea ice is virtually absent, the response is much weaker.

3.2 European mid-latitude response

3.2.1 Strong PI maritime cloud albedo effect leads to continental cooling during winter

Unlike the Arctic, where we model a clear winter warming across the different climate states considered in this study, the wintertime surface air temperature response at the European mid-latitudes varies considerably depending on the climate state. We model slight warming or an ambiguous temperature response in the PD and Ft simulations but significant cooling under PI conditions (Fig. 4f). This PI mid-latitude cooling extends into south-western Asia and is also visible in eastern North America (Figs. 1a to 1c).

As discussed in previous sections, we generally model a stronger cloud response to the volcanic aerosol perturbations under PI conditions compared to PD and Ft. We would further expect a stronger response over open oceans compared to continents as oceanic clouds are in general less polluted (e.g., Rosenfeld et al., 2014). Indeed, this gives rise to strong PI cloud albedo effect in our simulations, in particular over the northern Atlantic and Pacific Oceans, along with the Mediterranean, Black, and Caspian Seas (Supplementary Fig. S2). The resulting decrease in incoming sunlight leads to surface cool-

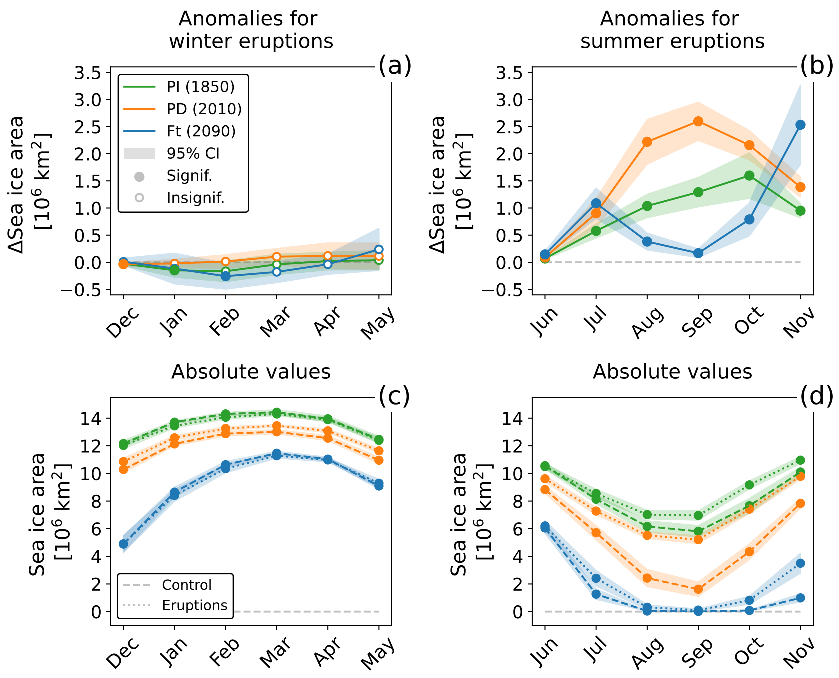

Figure 3. Monthly mean Arctic sea ice area anomalies for eruptions starting in December (a) and June (b), and corresponding control means (c and d). Bullets indicate ensemble means and shades 95% confidence intervals (CI) based on a two-tailed t-test. Filled bullets are used to highlight significance. Solid lines in (a) and (b) indicate anomalies. Dashed and dotted lines in (c) and (d) indicate absolute values from the control and eruption simulations respectively.

ing over these water bodies (Fig. 1a) which is then advected across the Eurasian and North American continents with the westerlies (winds not shown here).

Large Icelandic eruptions, which had substantial effusive components, have been connected to anomalously cold winters in pre-industrial Europe (Oppenheimer et al., 2018; Zambri et al., 2019; Gabriel et al., 2024). This is in agreement with our simulations. However, our simulations indicate that were similar eruptions to happen today or in the near future, the climate response would be considerably different. Instead of winter cooling we might expect no discernible temperature response at the European mid-latitudes, or even a slight warming, due to weaker PD and Ft cloud response to the volcanic aerosol perturbations.

3.2.2 Summer cooling insensitive to climate state

At the European mid-latitudes, we model a clear increase in SO_4 aerosol column burden anomalies going from PI to PD to Ft climate states during the summer months (Fig. 4a) as a result of increased levels of tropospheric oxidants (Supplementary Fig. S3). However, due to the much lower SO_4 aerosol background load under PI conditions (Fig. 4g), we model the strongest cloud response in the PI simulations (Figs. 4b to 4d). This leads to relatively strong cloud-radiation and weak aerosol-radiation effects under PI conditions compared to PD and Ft conditions, resulting in almost the same surface radiative forcing (Fig. 4e) and surface air temperature (Fig. 4f) anomalies for these three climate states.

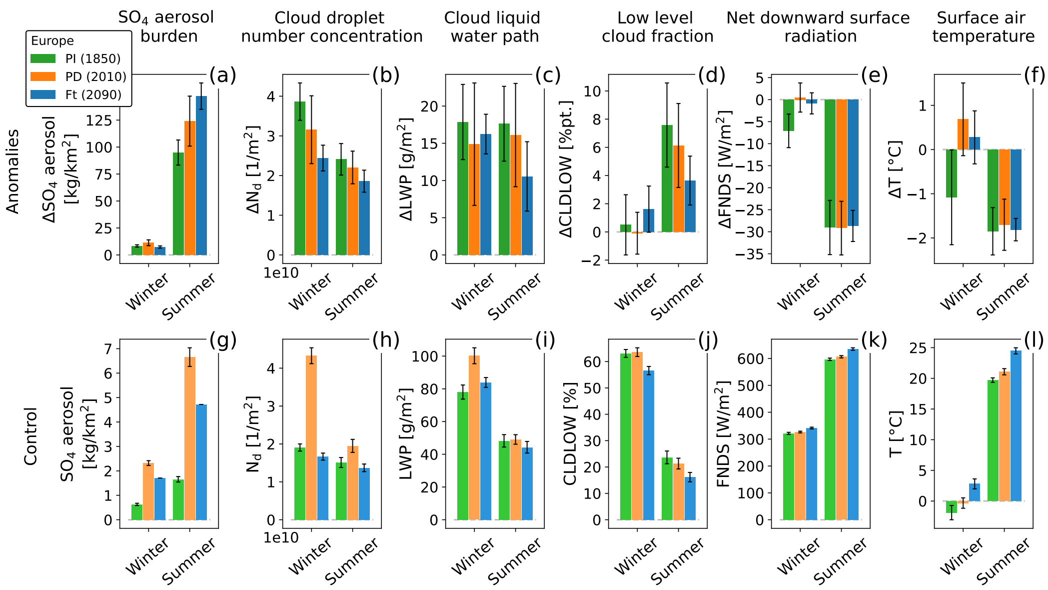

Figure 4. Same as Fig. 2 but averaged over European mid-latitudes as defined by 40°N to 65°N and 10°W to 60°E, land only.

4 Summary and conclusions

In this study we simulate the climate impacts of large and long-lasting high-latitude, effusive volcanic eruptions under different climate states, corresponding to pre-industrial, present day, and future conditions. For the last case, we assume high anthropogenic greenhouse gas and aerosol emissions, following SSP3-7.0. Our main results are as follows:

- During winter, we find that the surface warming in the Arctic is strongly modulated by the background cloud state, as the longwave radiation trapping abilities of clouds strongly depend on their liquid water content, with greater warming under the drier and colder pre-industrial conditions compared to the wetter and warmer present day and future conditions.
- During summer, we find that the sea ice area significantly modulates the surface cooling in the Arctic across climate states. More Arctic sea ice in the pre-industrial simulations results in weaker surface cooling, and less sea ice in the present day and future simulations results in stronger cooling.
- Increased shortwave cloud shielding as a result of volcanic aerosol perturbations leads to significantly greater sea ice area in the Arctic during summer and fall following an eruption starting in June across climate states. This effect is the strongest in areas where partial sea ice cover is maintained, but weaker in areas which are either completely ice covered or ice free.
- During winter, we find a disproportionally strong pre-industrial cloud albedo response over the mid-latitude oceans. The resulting surface cooling is then passed over the continents with the westerlies, leading to winter cooling. This is contrasted by slight warming or an ambiguous temperature response over the European mid-latitudes in present day and future climates.
- Despite clean clouds being more susceptible to aerosol perturbations than polluted clouds, we model similar surface air temperature response during summer at the European mid-latitudes across the climate states considered in this study. The reason is a considerably stronger direct aerosol effect under present day and future conditions as a result of higher levels of atmospheric oxidants.

The different surface air temperature responses in the Arctic between different climate states are rather due to a warmer climate as a result of anthropogenic greenhouse gas emissions, with subsequent changes in cloud properties (during winter) and decreased sea ice (during summer), than changes in the background aerosol state. Conversely, at the mid-latitudes, the background aerosol state is the dominant modulator.

These findings indicate that although the climate impacts of past volcanic eruptions can serve as analogues for the climate response to similar present day or future eruptions, there are important distinctions. Most notably during winter where we model very different responses between pre-industrial conditions on one hand and present day and future on the other, both in the Arctic and at the mid-latitudes.

Our results further highlight how volcanically induced increase in cloud shielding has the potential to help maintain Arctic sea ice during summer and fall in a warming climate. This last point is especially relevant for sea ice dependent ecosystems (e.g., Vincent & Mueller, 2020) and, due the similarities between effusive volcanic eruptions and climate intervention in the form of cloud seeding, provides a motivation for further studies into small scale climate modification with the aim of preserving biological diversity under the ongoing anthropogenic climate change.

Open Research

The CESM2(CAM6) output underlying the results and figures presented in this paper, along with a Jupyter Notebook containing plotting scripts for the figures, are available at the NIRD Research Data Archive (Zoëga, 2025).

Acknowledgments

This project received funding from the European Union's Horizon 2020 research and innovation program under the Marie Skłodowska-Curie grant agreement No. 945371 through the "CompSci: Training in Computational Science" doctoral program launched and managed by the Faculty of Mathematics and Natural Sciences at the University of Oslo. TS further acknowledges funding from the European Research Council under grant No. 101045273 ("STEP-CHANGE"). KK further acknowledges funding from the Research Council of Norway/University of Oslo Toppforsk project "VIKINGS" with the grant No. 275191. The simulations in this study were performed on the Fram high performance computer and the model output stored on the National Infrastructure for Research Data (NIRD), both provided by Sigma2 and the Norwegian Research Infrastructure Services (NRIS) in Norway.

References

Albrecht, B. A. (1989). Aerosols, cloud microphysics, and fractional cloudiness. *Science*, *245*(4923), 1227–1230. doi: 10.1126/science.245.4923.1227

Barlow, R. J. (1993). *Statistics: a guide to the use of statistical methods in the physical sciences* (Vol. 29). John Wiley & Sons.

Bates, T., Lamb, B., Guenther, A., Dignon, J., & Stoiber, R. (1992). Sulfur emissions to the atmosphere from natural sources. *Journal of Atmospheric Chemistry*, *14*, 315–337. doi: 10.1007/BF00115242

Bonny, E., Thordarson, T., Wright, R., Höskuldsson, A., & Jónsdóttir, I. (2018). The volume of lava erupted during the 2014 to 2015 eruption at Holuhraun, Iceland: A comparison between satellite-and ground-based measurements. *Journal of Geophysical Research: Solid Earth*, *123*(7), 5412–5426. doi: 10.1029/2017JB015008

Breen, K. H., Barahona, D., Yuan, T., Bian, H., & James, S. C. (2021). Effect of volcanic emissions on clouds during the 2008 and 2018 Kilauea degassing events. *Atmospheric Chemistry and Physics*, *21*(10), 7749–7771. doi: 10.5194/acp-21-7749-2021

Chen, Y., Haywood, J., Wang, Y., Malavelle, F., Jordan, G., Partridge, D., ... others (2022). Machine learning reveals climate forcing from aerosols is dominated by increased cloud cover. *Nature Geoscience*, *15*(8), 609–614. doi: 10.1038/s41561-022-00991-6

Comiso, J. C., Bliss, A. C., Gersten, R., Parkinson, C. L., & Markus, T. (2024). *Current State of Sea Ice Cover.* Retrieved 2014-09-12, from `https://earth.gsfc.nasa.gov/cryo/data/current-state-sea-ice-cover`

Danabasoglu, G., Lamarque, J.-F., Bacmeister, J., Bailey, D., DuVivier, A., Edwards, J., ... others (2020). The Community Earth System Model Version 2 (CESM2). *Journal of Advances in Modeling Earth Systems*, *12*(2), e2019MS001916. doi: 10.1029/2019MS001916

Eyring, V., Bony, S., Meehl, G. A., Senior, C. A., Stevens, B., Stouffer, R. J., & Taylor, K. E. (2016). Overview of the Coupled Model Intercomparison Project Phase 6 (CMIP6) experimental design and organization. *Geoscientific Model Development*, *9*(5), 1937–1958. doi: 10.5194/gmd-9-1937-2016

Gabriel, I., Plunkett, G., Abbott, P. M., Behrens, M., Burke, A., Chellman, N., ... others (2024). Decadal-to-centennial increases of volcanic aerosols from Iceland challenge the concept of a Medieval Quiet Period. *Communications earth & environment*, *5*(1), 194. doi: 10.1038/s43247-024-01350-6

Gettelman, A., Mills, M., Kinnison, D., Garcia, R., Smith, A., Marsh, D., ... others (2019). The whole atmosphere community climate model version 6

(WACCM6). *Journal of Geophysical Research: Atmospheres*, *124*(23), 12380–12403. doi: 10.1029/2019JD030943

Gettelman, A., & Morrison, H. (2015). Advanced two-moment bulk microphysics for global models. Part I: Off-line tests and comparison with other schemes. *Journal of Climate*, *28*(3), 1268–1287. doi: 10.1175/JCLI-D-14-00102.1

Gryspeerdt, E., Goren, T., Sourdeval, O., Quaas, J., Mülmenstädt, J., Dipu, S., ... Christensen, M. (2019). Constraining the aerosol influence on cloud liquid water path. *Atmospheric Chemistry and Physics*, *19*(8), 5331–5347. doi: 10.5194/acp-19-5331-2019

Hjartarson, Á. (1988). Þjórsárhraunið mikla - stærsta nútímahraun jarðar. *Náttúrufræðingurinn*, *58*(1), 1–16. (In Icelandic with an English abstract)

Hunke, E. C., Lipscomb, W. H., Turner, A. K., Jeffery, N., & Elliott, S. (2013, December). *CICE: The Los Alamos Sea ice model documentation and software user's manual version 5.0* (Tech. Rep. No. LA-CC-06-012). Los Alamos NM 87545: Los Alamos National Laboratory.

Li, J., Carlson, B. E., Yung, Y. L., Lv, D., Hansen, J., Penner, J. E., ... others (2022). Scattering and absorbing aerosols in the climate system. *Nature Reviews Earth & Environment*, *3*(6), 363–379. doi: 10.1038/s43017-022-00296-7

Liu, X., Ma, P.-L., Wang, H., Tilmes, S., Singh, B., Easter, R., ... Rasch, P. (2016). Description and evaluation of a new four-mode version of the Modal Aerosol Module (MAM4) within version 5.3 of the Community Atmosphere Model. *Geoscientific Model Development*, *9*(2), 505–522. doi: 10.5194/gmd-9-505-2016

Lohmann, U., & Feichter, J. (2005). Global indirect aerosol effects: a review. *Atmospheric Chemistry and Physics*, *5*(3), 715–737. doi: 10.5194/acp-5-715-2005

Malavelle, F. F., Haywood, J. M., Jones, A., Gettelman, A., Clarisse, L., Bauduin, S., ... others (2017). Strong constraints on aerosol–cloud interactions from volcanic eruptions. *Nature*, *546*(7659), 485–491. doi: 10.1038/nature22974

Murray-Watson, R. J., & Gryspeerdt, E. (2022). Stability-dependent increases in liquid water with droplet number in the Arctic. *Atmospheric Chemistry and Physics*, *22*(9), 5743–5756. doi: 10.5194/acp-22-5743-2022

O'Neill, B. C., Tebaldi, C., Van Vuuren, D. P., Eyring, V., Friedlingstein, P., Hurtt, G., ... others (2016). The scenario model intercomparison project (ScenarioMIP) for CMIP6. *Geoscientific Model Development*, *9*(9), 3461–3482. doi: 10.5194/gmd-9-3461-2016

Oppenheimer, C., Orchard, A., Stoffel, M., Newfield, T. P., Guillet, S., Corona, C., … Büntgen, U. (2018). The Eldgjá eruption: timing, long-range impacts and influence on the Christianisation of Iceland. *Climatic Change*, *147*, 369–381. doi: 10.1007/s10584-018-2171-9

Rosenfeld, D., Andreae, M. O., Asmi, A., Chin, M., de Leeuw, G., Donovan, D. P., … others (2014). Global observations of aerosol-cloud-precipitation-climate interactions. *Reviews of Geophysics*, *52*(4), 750–808. doi: 10.1002/2013RG000441

Satheesh, S., & Moorthy, K. K. (2005). Radiative effects of natural aerosols: A review. *Atmospheric Environment*, *39*(11), 2089–2110. doi: 10.1016/j.atmosenv.2004.12.029

Schmidt, A., Carslaw, K., Mann, G., Rap, A., Pringle, K., Spracklen, D., … Forster, P. (2012). Importance of tropospheric volcanic aerosol for indirect radiative forcing of climate. *Atmospheric Chemistry and Physics*, *12*(16), 7321–7339. doi: 10.5194/acp-12-7321-2012

Shiogama, H., Fujimori, S., Hasegawa, T., Hayashi, M., Hirabayashi, Y., Ogura, T., … Takemura, T. (2023). Important distinctiveness of SSP3–7.0 for use in impact assessments. *Nature Climate Change*, *13*(12), 1276–1278. doi: 10.1038/s41558-023-01883-2

Shupe, M. D., & Intrieri, J. M. (2004). Cloud radiative forcing of the Arctic surface: The influence of cloud properties, surface albedo, and solar zenith angle. *Journal of climate*, *17*(3), 616–628. doi: 10.1175/1520-0442(2004)017<0616:CRFOTA>2.0.CO;2

Sigl, M., Toohey, M., McConnell, J. R., Cole-Dai, J., & Severi, M. (2022). Volcanic stratospheric sulfur injections and aerosol optical depth during the Holocene (past 11 500 years) from a bipolar ice-core array. *Earth System Science Data*, *14*(7), 3167–3196. doi: 10.5194/essd-14-3167-2022

Slingo, A., Brown, R., & Wrench, C. (1982). A field study of nocturnal stratocumulus; III. High resolution radiative and microphysical observations. *Quarterly Journal of the Royal Meteorological Society*, *108*(455), 145–165. doi: 10.1002/qj.49710845509

Small, J. D., Chuang, P. Y., Feingold, G., & Jiang, H. (2009). Can aerosol decrease cloud lifetime? *Geophysical Research Letters*, *36*(16). doi: 10.1029/2009GL038888

Stroeve, J. C., Serreze, M. C., Holland, M. M., Kay, J. E., Malanik, J., & Barrett, A. P. (2012). The Arctic's rapidly shrinking sea ice cover: a research synthesis. *Climatic change*, *110*, 1005–1027. doi: 10.1007/s10584-011-0101-1

Thordarson, T., & Hartley, M. (2015). Atmospheric sulfur loading by the ongoing Nornahraun eruption, North Iceland. In *EGU General Assembly Conference Abstracts* (p. 10708).

Thordarson, T., Miller, D., Larsen, G., Self, S., & Sigurdsson, H. (2001). New estimates of sulfur degassing and atmospheric mass-loading by the 934 AD Eldgjá eruption, Iceland. *Journal of Volcanology and Geothermal Research*, *108*(1-4), 33–54. doi: 10.1016/S0377-0273(00)00277-8

Thordarson, T., & Self, S. (2003). Atmospheric and environmental effects of the 1783–1784 Laki eruption: A review and reassessment. *Journal of Geophysical Research: Atmospheres*, *108*(D1), AAC–7. doi: 10.1029/2001JD002042

Toll, V., Christensen, M., Quaas, J., & Bellouin, N. (2019). Weak average liquid-cloud-water response to anthropogenic aerosols. *Nature*, *572*(7767), 51–55. doi: 10.1038/s41586-019-1423-9

Twomey, S. (1977). The influence of pollution on the shortwave albedo of clouds. *Journal of the atmospheric sciences*, *34*(7), 1149–1152. doi: 10.1175/1520-0469(1977)034<1149:TIOPOT>2.0.CO;2

Vincent, W. F., & Mueller, D. (2020). Witnessing ice habitat collapse in the Arctic. *Science*, *370*(6520), 1031–1032. doi: 10.1126/science.abe4491

Wang, X., Mao, F., Zhu, Y., Rosenfeld, D., Pan, Z., Zang, L., … Gong, W. (2024). Hidden large aerosol-driven cloud cover effect over high-latitude ocean. *Journal of Geophysical Research: Atmospheres*, *129*(13), e2023JD039312. doi: 10.1029/2023JD039312

Wendler, G., Eaton, F. D., & Ohtake, T. (1981). Multiple reflection effects on irradiance in the presence of Arctic stratus clouds. *Journal of Geophysical Research: Oceans*, *86*(C3), 2049–2057. doi: 10.1029/JC086iC03p02049

Yuan, T., Remer, L., & Yu, H. (2011). Microphysical, macrophysical and radiative signatures of volcanic aerosols in trade wind cumulus observed by the A-Train. *Atmospheric Chemistry and Physics*, *11*(14), 7119–7132. doi: 10.5194/acp-11-7119-2011

Zambri, B., Robock, A., Mills, M. J., & Schmidt, A. (2019). Modeling the 1783–1784 Laki eruption in Iceland: 2. Climate impacts. *Journal of Geophysical Research: Atmospheres*, *124*(13), 6770–6790. doi: 10.1029/2018JD029553

Zoëga, T., Storelvmo, T., & Krüger, K. (2023). Arctic warming from a high latitude effusive volcanic eruption.
(PREPRINT (Version 1) available at Research Square) doi: 10.21203/rs.3.rs-3249183/v1

Zoëga, T., Storelvmo, T., & Krüger, K. (2024). Modelled surface climate response to Icelandic effusive volcanic eruptions: Sensitivity to season and size. *EGUsphere*, *2024*, 1–37. (PREPRINT available at EGUsphere preprint repository) doi: 10.5194/egusphere-2024-2651

Zoëga, T. (2025). *CESM2(CAM6) simulations for the manuscript "Climate state dependent response to high-latitude effusive volcanic eruptions" [Data set].* Norstore. doi: 10.11582/2025.00003

Supporting Information for “Climate state dependent response to high-latitude effusive volcanic eruptions”

Tómas Zoëga[1], Trude Storelvmo[1], Kirstin Krüger[1]

[1]Department of Geosciences, University of Oslo, Oslo, Norway

Contents of this file

1. Introduction

This document includes supporting figures for “Climate state dependent response to high-latitude effusive volcanic eruptions”. The data underlying the figures comes from the CESM2(CAM6) simulations described in the main text.

2. Supporting figures

Supporting Figs. S1, S2, and S3 can be found in the following pages.

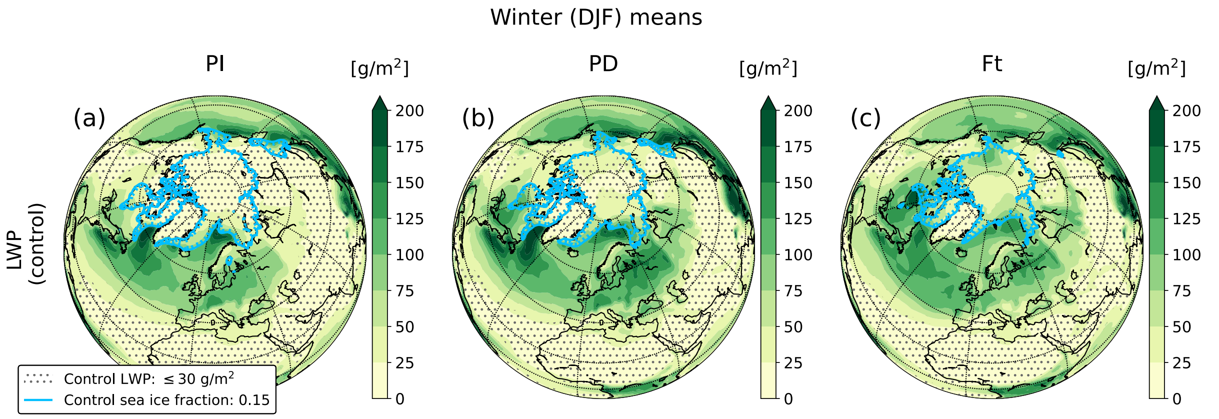

Figure S1. Liquid water path (LWP) from the control runs. December to February means. Areas with LWP ≤ 30 g/m^2 are dotted. Light blue contours indicate control sea ice edge as defined by 15% sea ice fraction.

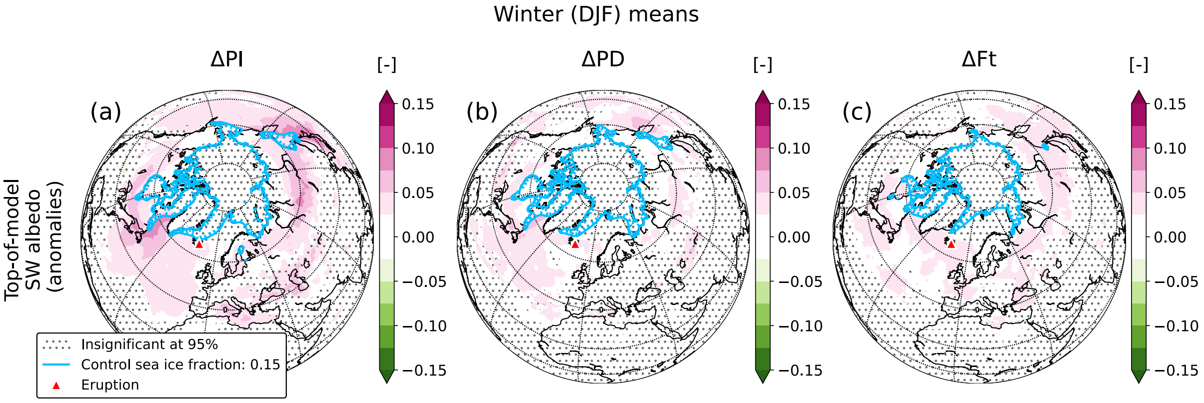

Figure S2. Top-of-model SW albedo anomalies for eruptions starting in December. December to February means. Dotted areas indicate insignificance at the 95% confidence level using a two-tailed t-test. Light blue contours indicate control sea ice edge as defined by 15% sea ice fraction.

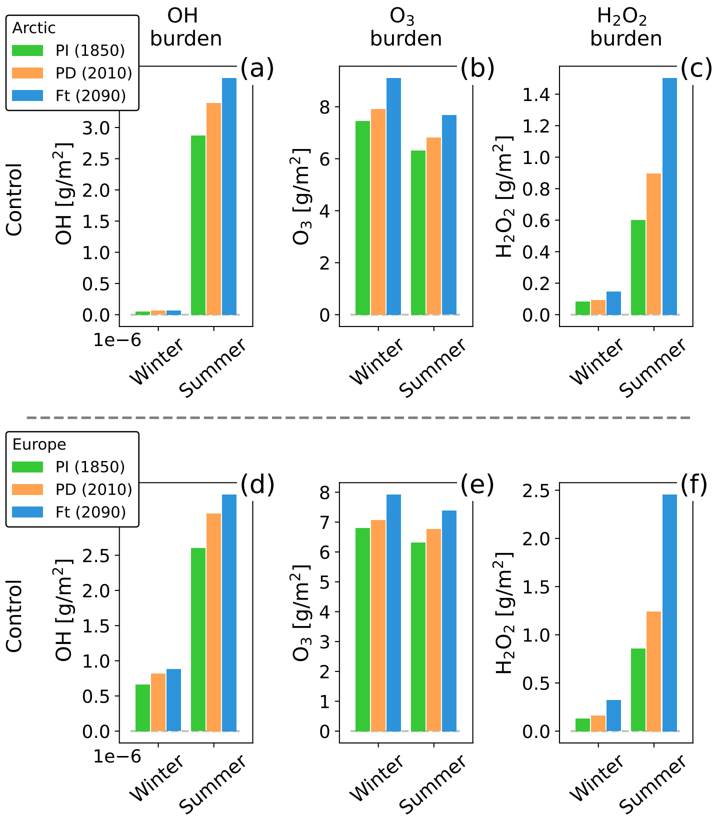

Figure S3. Arctic (a, b, c) and mid-latitude European (d, e, f) control means for the oxidants relevant for CESM2(CAM6)'s sulfur chemistry (OH, O_3, and H_2O_2) for the first three months of eruptions starting in December (winter, DJF) and June (summer, JJA). Green bars indicate pre-industrial (PI) conditions, orange present day (PD), and blue future (Ft). Here, the Arctic and the European mid-latitudes are defined as in Fig. 2 and Fig. 4 in the main text respectively. Note that OH and O_3 are prescribed.